

CHAPTER IV

EFFECT OF pH ON SORPTION AND TRANSPORT OF Pb^{2+} , Mn^{2+} , Zn^{2+} , and Ni^{2+} THROUGH LATERITIC SOIL: COLUMN EXPERIMENTS AND TRANSPORT MODELING

Abstract

This study investigated the effects of pH on the sorption and transport of Pb^{2+} , Mn^{2+} , Zn^{2+} , and Ni^{2+} through lateritic soil columns. Model results derived from CXTFIT for the symmetric breakthrough curves (BTCs) of bromide (Br^-) data suggested that physical nonequilibrium processes were absent in the uniformly packed columns. The heavy metals BTCs were asymmetrical and exhibited tailing phenomenon, indicating the presence of chemical nonequilibrium in the columns. The retardation factors of Pb^{2+} were the largest of the 4 metals at both pH 4 (33.26) and 5 (35.35). The retardation factors from largest to smallest were: $Pb^{2+} > Zn^{2+} > Mn^{2+} > Ni^{2+}$ for pH 4 and $Pb^{2+} > Zn^{2+} > Ni^{2+} > Mn^{2+}$ for pH 5. Use of Langmuir isotherm parameters from batch studies with HYDRUS-1D did not predict the BTCs well. When the BTCs were curve-fitted using linear and nonlinear Langmuir isotherm, and two-site model (TSM), the TSM described these heavy metal BTCs better than the equilibrium linear/nonlinear Langmuir model. The fraction of instantaneous site (f) of all metals on lateritic soil was consistently about 30-44 % of sorption site. Model results also suggested that Pb^{2+} was more strongly sorbed than others at both pH conditions.

Keywords: pH effect; heavy metals, HYDRUS-1D, two-site model

4.1 Introduction

Pollution from heavy metals is a very serious threat not only to environment but also to human health due to their toxicity and non-degradability. Heavy metals are generated from both anthropogenic and natural sources. Historically, mining industries is one of the major sources of heavy metal releases into the environment. One of the consequences of mining is acidic mine drainage (Moreno and Neretnieks, 2006; Sheoran and Sheoran, 2006) where water infiltrating through the metal sulphide minerals, waste rocks and seepage from tailing dams may result in heavy metals released into the surrounding soils and groundwater. According to previous studies, pH is one of the most significant factor that affects transport and sorption of heavy metals to soils (Mclean and Bledsoe, 1992; Mesquita and Vieira, 2002). Also, many mine soils when removed from the subsurface, are rapidly oxidized and become acidic, leaching large quantities of cations such as calcium, manganese, and iron. Many studies have focused on the sorption of heavy metals in soils under equilibrium conditions using batch sorption experiments (Gutierrez and Fuentes, 1991; Srivastava et al., 2005; Serrano et al., 2005, Arias et al., 2006). Another approach is to investigate transport of heavy metals in mine soils under using continuous flow column transport technique which usually better approximates the field conditions and may provide information that are not available using equilibrium batch experiments (Plassard et al., 2000; Pazka, 2003; Miretzky et al., 2006).

Pang et al. (2002) showed that the breakthrough curves of Cd, Zn, and Pb in gravel columns with pore water velocities ranging from 3 to 60 m/day displayed long tailing, suggesting that non-equilibrium occurred in the gravel columns resulting from increasing pore water velocity. Kookana and Naidu (1998) observed that movement of Cd increased nearly four times in Oxisol soil when the concentration of background electrolytes (NaNO_3) was increased from 0.03 M to 0.15 M. Although pH is one of the major factor affected sorption and transport of heavy metals, not many researches have investigated the effect of pH on sorption and transport of heavy metals using column technique, especially for mine soil. The Akara mining site is one of the gold mines in Thailand and it is active site generating vast masses of mine tailings which might be a major source of heavy metal contaminants in the future. Also, possibility of the acid mine drainage occurring at the site after mine closure in

high which lead to leaching out faster.

The objective of this research is investigate the effects of aqueous pH conditions on sorption and transport of heavy metal (Pb^{2+} , Zn^{2+} , Ni^{2+} , and Mn^{2+}) through lateritic soil found near the mine area. Soil column experiments were conducted to understand the sorption and transport of heavy metals from the mine tailings in lateritic soils. The breakthrough curves were then modeled using HYDRUS-1D model with both linear and Langmuir sorption model and equilibrium and non-equilibrium conditions.

4.2 Materials and Methods

4.2.1 Soil samples and reagents

Bulk lateritic soils were collected at the depth between 0-2 m below ground surface from Akara mine area. Soil samples were packed, transported back to the laboratory, and stored at 4°C prior to use. All samples were crushed, air-dried, and sieved through 2-mm mesh prior to soil characterization and sorption studies. Table 4.1 presents the lateritic soil physical-chemical properties. Soil texture and permeability were characterized using sieve and sedimentation methods (Allen, 1974), and falling head permeability method, respectively. Soil pH was measured in distilled water at 1:1 ratio of soil to water (Reeuwijk, 1995). Cation exchange capacity was measured using the 1 M NH_4OAc (pH 7) solution extraction method (Thomas, 1982), and the organic matter content was estimated by the Walkley and Black method (Walkley and Black, 1934). Soil specific surface area was determined using the BET method (Brunauer et al., 1938) using nitrogen (N_2) as the sorbate. The mineralogical composition of soil samples was determined using an X-ray fluorescence spectrophotometer. The four metals (Pb^{2+} , Zn^{2+} , Ni^{2+} and Mn^{2+}) were prepared by dissolving amounts of $\text{Pb}(\text{NO}_3)_2(\text{s})$, $\text{Zn}(\text{NO}_3)_2 \cdot 6\text{H}_2\text{O}(\text{s})$, $\text{Ni}(\text{NO}_3)_2 \cdot 6\text{H}_2\text{O}(\text{s})$, and $\text{MnCl}_2 \cdot 4\text{H}_2\text{O}(\text{s})$ in distilled water to obtain 0.1 mol L^{-1} solution. A buffer solution containing 0.01 M NaAc (CH_3COONa ; $pK_a = 4.76$, $MW = 136.08 \text{ g mol}^{-1}$) was used as the aqueous phase. NaOH and HNO_3 were used for the pH adjustments to maintain pH 4 and 5. All the glassware used for dilution, storage and experiments were cleaned with non-ionic detergent, thoroughly rinsed with tap water, soaked overnight

in a 10% (v/v) HNO₃ solution and finally rinsed with ultrapure quality water before use. (Miretzky et al., 2006)

Table 4.1 Physical-chemical properties of Akara lateritic soil

Property	value
pH	5.3
Organic matter (%)	0.16
Clay fraction (%)	53.8
Silt fraction (%)	24.4
Sand fraction (%)	21.8
CEC (cmol kg ⁻¹)	28.8
Specific surface area (m ² g ⁻¹)	48.69
Bulk density (g cm ⁻³)	1.23
Specific gravity (-)	2.71
Hydraulic conductivity (cm hr ⁻¹)	3.17
Bulk chemical composition	
SiO ₂	48.41
Al ₂ O ₃	40.58
Fe ₂ O ₃	7.93
K ₂ O	0.82
CaO	0.85
MgO	0.58

4.2.2 Tracer and heavy metals transport experiments

The columns (see Figure 4.1) used throughout the experiment were acrylic tubes with a length of 10 cm and an internal diameter of 2.5 cm. The lateritic soil were packed into the columns by using a wet packing technique where the slurry of lateritic soil (soil:water ratio of 1.3:1) were added with increment of every 0.5 cm deep. The bottom cap consisted of an acrylic plate with small holes, covered with fine mesh of 0.15 mm. to distribute the inflow. The soil column was maintained at 8 mL hr⁻¹ using piston pump. The column experiments were conducted at room

temperature ($25^{\circ}\text{C} \pm 1$). The soil column was initially saturated from the bottom with deionized water and at least 6 pore volumes (PVs) of deionized water was pumped through the column at a rate of 8 mL hr^{-1} using a piston pump eliminate entrapped air and to minimise the possibility of preferential flow (Pang et al., 2004). After the saturation procedure, distilled water containing 30 mg L^{-1} of bromide (Br^{-}) at a rate of 8 mL hr^{-1} was injected from the bottom. Column effluent was collected using a fraction collector. The effluents were filtered and then analyzed for bromide using Ion chromatography (IC). After the test, about 6 PVs of the buffer solution was injected to establish the pH of the column. When the pH of soil column was constant as measured in the effluent from the column, metal solutions (Pb^{2+} , Mn^{2+} , Zn^{2+} , and Ni^{2+}) at a concentration of 5 mmol L^{-1} was injected from bottom. The effluent was collected every 1 hour with a fraction collector. During the injection, samples were taken from the test solution periodically to monitor influent concentrations of metals and pH. The metal concentrations in the effluent were determined by flame atomic absorption spectrophotometry (FAAS). The breakthrough curves (BTC), expressed as the relative concentrations (C/C_0) and pore volume (V/V_0), where C_0 is the initial concentration added and V_0 is the pore volume of soil column, were plotted. Several column tests were duplicated to assure the consistency of column packing and reproducibility of the experiments.

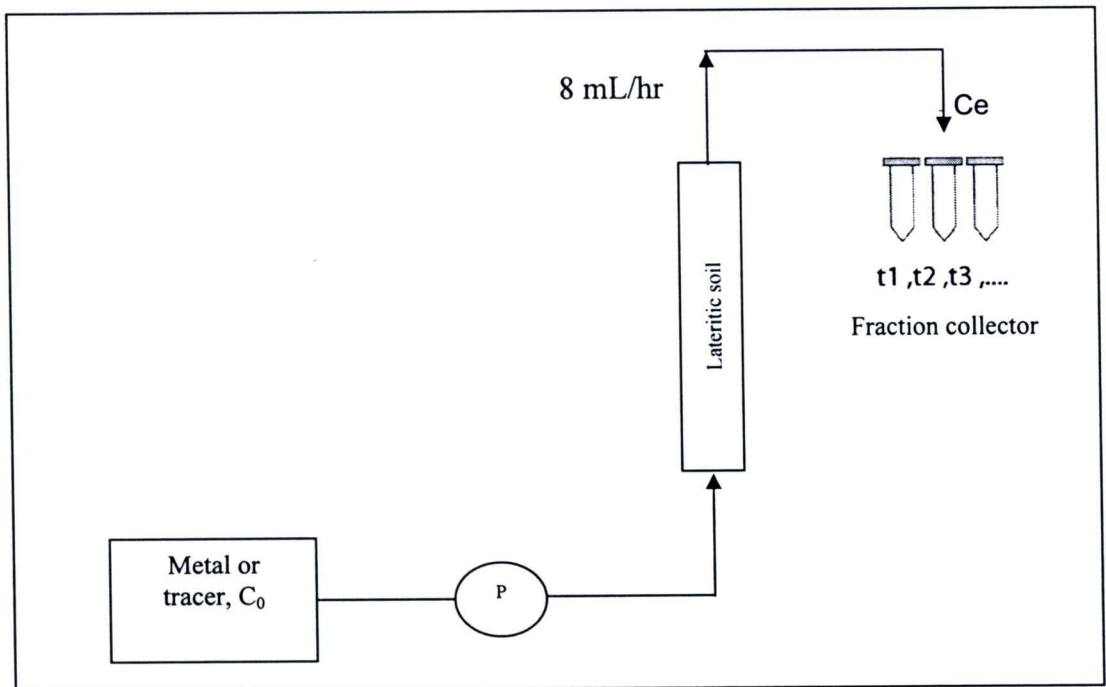


Figure 4.1 Schematic design of column experiment

Table 4.2 Column studies for single metal for different pH

Metal	Concentration (mmol L ⁻¹)	pH
Pb ²⁺	5	4 and 5 ^{*,±}
Mn ²⁺	5	4 and 5 [±]
Ni ²⁺	5	4 [*] and 5
Zn ²⁺	5	4 and 5



*duplicate tests conducted after the column tests were completed

±the tracer test was done before the Mn²⁺ test at pH 5, Pb²⁺ at pH 5, and Pb²⁺ (5 mM) - Ni²⁺ (3 Mm) at pH 5 (Duplicate column) in chapter 5

4.2.3 Area method

The breakthrough data of the heavy metal studies were analyzed to determine the retardation factors (R) of each metal onto soils. This was determined by the area method (Nkedi-Kizza et al., 1987). The retardation factors were calculated as:

$$R_{area} = PV_1 - \sum_{i=0}^{PI_1} (C/C_0) \Delta PV \quad (1)$$

where C is the effluent concentration, C_0 is the influent concentration, and PV_1 is the number of the pore volume at which the relative concentration is 1.0.

4.2.4 Transport models

CXTFIT model was used to simulate the transport of conservative tracer to examine any stagnant (mmobile) water in the columns and used the HYDRUS-1D model was used to evaluate linear/nonlinear equilibrium and chemical nonequilibrium processes of heavy metal sorption and transport in the columns.

(a) CXTFIT

CXTFIT 2.0 (Torride et al., 1995) is a program presenting a number of analytical solutions for a one-dimensional transport model based on the convection-dispersion equation (CDE). CXTFIT includes an inverse modeling capability that uses a nonlinear least-squares parameter optimization method. The program solves the inverse problem by fitting mathematical solutions of the theoretical transport model to experimental data. The equilibrium CDE may be written as:

$$\frac{\partial C}{\partial t} = D_L \frac{\partial^2 C}{\partial x^2} - v_x \frac{\partial C}{\partial x} - \frac{\rho}{\theta} \frac{\partial C^*}{\partial t} \pm \left[\frac{\partial C}{\partial t} \right]_{rxn} \quad (2)$$

where C = concentration of solute in liquid phase (mg L^{-1}); t = time (hr); D_L = longitudinal dispersion coefficient ($\text{cm}^2 \text{hr}^{-1}$); v_x = average linear groundwater velocity (cm hr^{-1}); ρ = bulk density of aquifer (g cm^{-3}); θ = volumetric moisture content or porosity for saturated media; C^* = amount of solute sorbed per unit weight of solid (mg g^{-1}); rxn = subscript indicating a biological or chemical reaction of the solute (other than sorption) ($\text{mg L}^{-1} \text{hr}^{-1}$)

Depending on the equilibrium-nonequilibrium assumptions for C^* , CXTFIT 2.0 use a deterministic equilibrium CDE model, noted as CD_{eq} , or CXTFIT 2.0 deterministic two-region nonequilibrium model, noted as TRM. These models describe the sorption of the solute by a linear sorption isotherm. In this study, CXTFIT was used to assess the transport parameters by using linear equilibrium CDE model (CD_{eq}) and two-region nonequilibrium model (TRM) to evaluate any physical nonequilibrium processes in the system. In the two-region model, the physical nature of the porous medium is separated into two domains: a mobile “dynamic” domain, and an immobile “stagnant” domain. Solute movement in the mobile region occurs by convection-dispersion model, whereas solute exchange between the two regions occurs by the first order diffusion. The governing equation for the two-region nonequilibrium model is:

$$(\theta_m + fpK_d) \frac{\partial c_m}{\partial t} + [\theta_{im} + (1-f)\rho K_d] \frac{\partial c_{im}}{\partial t} = \theta_m D_m \frac{\partial^2 c_m}{\partial x^2} - q \frac{\partial c_m}{\partial x} \quad (3)$$

$$[\theta_{im} + (1-f)\rho K_d] \frac{\partial c_{im}}{\partial t} = \alpha (c_m - c_{im}) \quad (4)$$

where the subscripts m and im refer to the mobile and immobile regions, respectively; α is a first-order mass transfer coefficient (d^{-1}), representing the rate of solute exchange between the mobile and immobile regions; and f is the fraction of mobile water. For nonsorbing solutes such as bromide (Br^-), values of β and ω can be used to evaluate potential contributions from physical nonequilibrium. Values for these nonequilibrium terms from the two-region model can be described as:

$$\beta = \frac{\theta_m + fpK_d}{\theta + \rho K_d} \quad (5)$$

$$\omega = \frac{\alpha L}{q} \quad (6)$$

It should be noted that the sorption parameters obtained from CXTFIT program correspond to the K_d values of the from linear isotherm. However, sorption is generally not linear for heavy metals. Therefore, the HYDRUS-1D was applied to evaluate metal sorption and transport in the columns.

(b) HYDRUS-1D

HYDRUS-1D model can be used to simulate transport of heavy metals in soils and the model code can be applied for different equilibrium and non-equilibrium flow and transport in both direct and inverse mode. The following transport model were used in this study to assess the experimental breakthrough curves (BTCs):

- Linear sorption model and nonlinear Langmuir sorption model for the equilibrium convection-dispersion transport model (Eq.2)
- Chemical non-equilibrium model or the two-site model (TSM) as

presented (Eq.7) Selim et al. (1976). Using Langmuir sorption model, the governing equation for the two-site model becomes (Fetter, 1993):

$$\left(1 + \frac{f\rho}{\theta} \left[\frac{Q_{\max} b}{(1 + bC)^2} \right] \right) \frac{\partial c}{\partial t} = D \frac{\partial^2 c}{\partial x^2} - v \frac{\partial c}{\partial x} - \frac{\alpha\rho}{\theta} \left[(1-f) \frac{Q_{\max} bC}{1 + bC} - s_2 \right] \quad (7)$$

where f is the fraction of equilibrium sites and α is a first-order kinetic rate coefficient (d^{-1}). S_2 is solid phase concentration at site 2. The numerical solution in the HYDRUS-1D code (Šimůnek et al., 2008) was used to optimize the sorption constant, the Langmuir component (Q_{\max} , b), the rate coefficient (α), and the fraction of equilibrium sites (f)

4.2.5 Parameter estimation

The hydrodynamic dispersion coefficient D of the soil was estimated from the bromide BTCs using the nonlinear least-squares parameters optimization method (inverse model routine) in CXTFIT (Toride et al., 1999). The equilibrium convection-dispersion (CDeq) model with R set to 1 and the two-region nonequilibrium convection-dispersion was applied to examine any physical nonequilibrium processes in the system. The hydrodynamic dispersion coefficient estimated from the bromide BTC was then used to estimate the soil dispersivity, $\lambda = D/v$. The average dispersivity (λ_{avg}) of 3 bromide BTCs was used to further describe the behavior of heavy metal BTCs, which was introduced in convection-dispersion model of HYDRUS-1D (Šimůnek et al., 2008) to estimate sorption parameters of heavy metals under different pH conditions using linear and nonlinear sorption isotherm models. Also, the chemical nonequilibrium model (2-site model, TSM) was used to estimate the sorption parameters (Q_{\max} and b in case of Langmuir isotherm) and nonequilibrium parameters (f and α) for transport of heavy metals. Least square errors (SSEs) were used to determine the appropriateness of the curve fitting. In addition, column-determined sorption coefficients was compared with batch-determined sorption coefficients from the previous work done by Putthividhya and Chotpantararat (2007)

4.3 Results and discussion

4.3.1 Bromide Breakthrough Curves

The best CXTFIT model fits for the equilibrium and the two-region nonequilibrium model are presented in Figure 4.1. The estimated column parameters are presented in Table 4.3. All bromide BTCs are symmetrical indicating that equilibrium transport occurred in the columns. Moreover, the results of the two-region nonequilibrium model for the bromide BTCs gave β values of 1 and ω values of 100, suggesting that all the water in the system was mobile and the equilibrium model should be used for analyzing the bromide data (Beigel and Pietro, 1999; Pang et al., 2002). Comparison of the experimental results of the bromide BTCs (Figure 4.1 and Table 4.3) showed that there were no significant differences in the dispersivity values. The average values of the dispersivity from the three columns were used in subsequent modeling of heavy metals BTCs. The average dispersivity, λ_{avg} , obtained from CXTFIT program was equal to 1.42 cm.

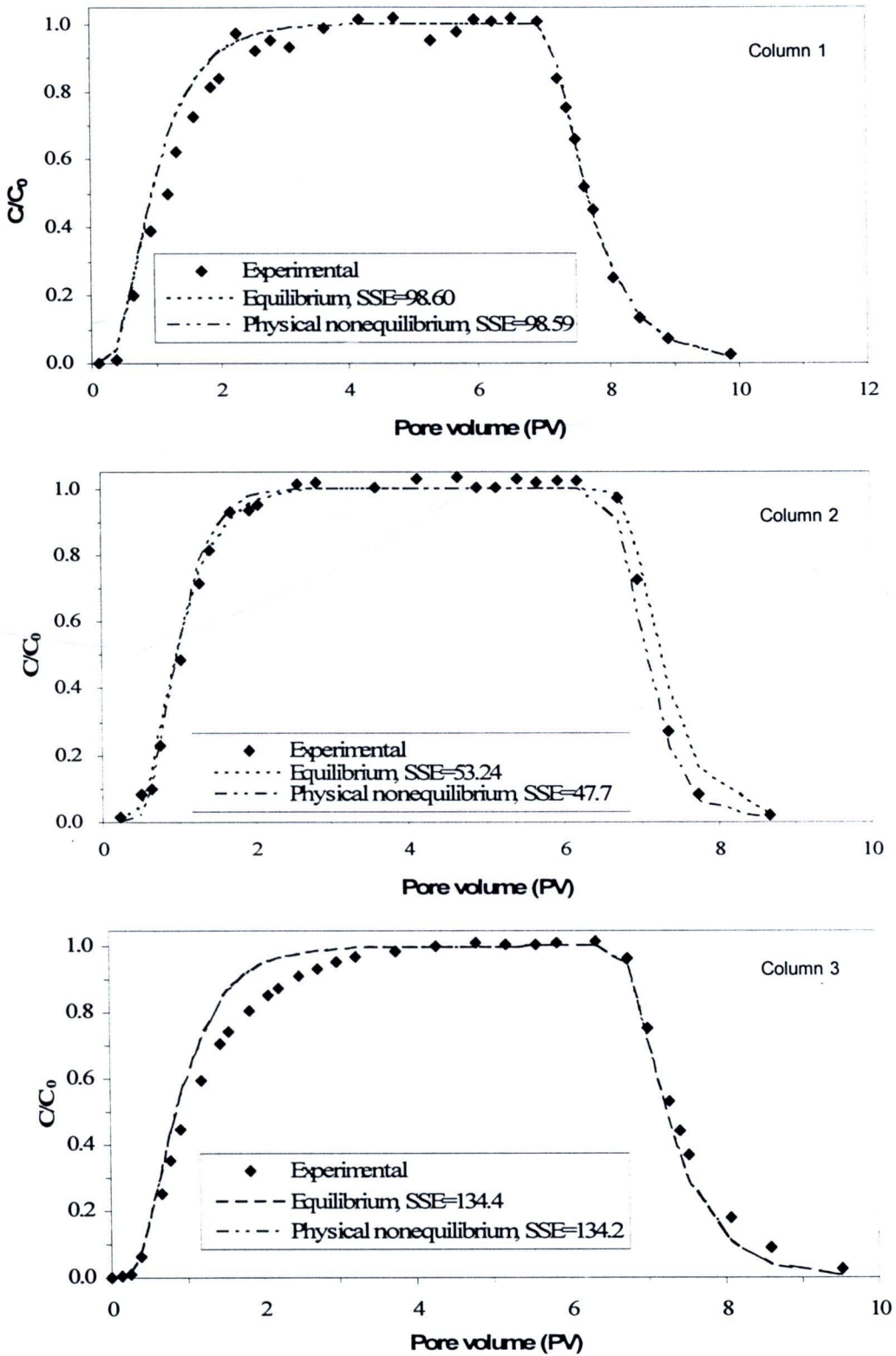


Figure 4.2 Experimental and CXTFIT-simulated concentrations of breakthrough curves of bromide

Table 4.3 Equilibrium convection-dispersion (CD_{eq}) and two-region model (physical non-equilibrium model) parameter values estimated from the bromide data.

Experimental conditions		CD_{eq}			Two-region model				
Column	Measured v ($cm\ hr^{-1}$)	D^* ($cm^2\ hr^{-1}$)	λ	SSE	D^* ($cm^2\ hr^{-1}$)	λ	β^*	ω	SSE
1	2.54	4.71±1.16	1.73±0.49	98.86	4.48±1.19	1.76±0.47	1±0.93	100	98.81
2	2.60	2.49±0.64	0.96±0.25	53.24	1.79±0.48	0.69±0.18	1±0.66	100	47.70
3	2.64	4.15±1.53	1.57±0.58	134.4	4.15±1.65	1.57±0.58	1±1.20	100	134.2

[†]Estimated value ± 95% confidence interval

4.3.2 Metal transport- Experimental results

Figures 4.2 and 4.3 show the BTCs for four metals under different pH conditions. Table 4.4 shows the properties of the columns used in heavy metal column studies. The Ni^{2+} column at pH 4 and Pb^{2+} column at pH 5 were chosen for duplicate column test as the retardation factor for these had the lowest and highest retardation factor, respectively.

4.3.2.1 Effect of pH on retention of heavy metals

The retardation factors (Table 4.4) were estimated using the area methods (Maraqa, M.A. 2001) and the retardation factors of Pb^{2+} were the largest at both pH 4 (33.26) and 5 (35.35). The retardation factors reveal the following trend: Pb^{2+} (33.26) > Zn^{2+} (19.61) > Mn^{2+} (17.90) > Ni^{2+} (11.21 and 11.22 (duplicate sample)) for pH 4 and Pb^{2+} (35.35 and 38.71 (duplicate sample)) > Zn^{2+} (30.15) > Ni^{2+} (28.65) > Mn^{2+} (19.22) for pH 5. The retardation factors were similar to retardation factor of Taoyuan soil: Cd^{2+} (37.10) > Zn^{2+} (30.28) > Ni^{2+} (27.52) (Liu et al., 2006) and of the lateritic soil: Cr^{3+} (98) > Pb^{2+} (50) > Zn^{2+} (17) ~ Ni^{2+} (16) > Cd^{2+} (10) (Chalermyanont et al., 2008).

Schwertmann and Taylor (1989) found that sequence of the retention of heavy metals for goethite was in the order $Cu > Pb > Zn > Cd > Co > Ni > Mn$, while hematite gave the same sequence except for an exchange in position of Cu and Pb. Gomes et al. (2001) investigated the distribution coefficients of heavy metals for

seven agriculture soils and found that the most common sequences of the distribution coefficient were $\text{Cr} > \text{Pb} > \text{Cu} > \text{Cd} > \text{Zn} > \text{Ni}$ and $\text{Pb} > \text{Cr} > \text{Cu} > \text{Cd} > \text{Ni} > \text{Zn}$. The sequences of retention of other studies were similar to the sequence of retention for the column studies: $\text{Pb}^{2+} > \text{Zn}^{2+} > \text{Mn}^{2+} > \text{Ni}^{2+}$. The trend is also in line with the sorption capacity for this soil (Table 4.4) showing the highest sorption capacity in the order of $\text{Pb}^{2+} > \text{Zn}^{2+} > \text{Mn}^{2+} > \text{Ni}^{2+}$ for pH 4 and $\text{Pb}^{2+} > \text{Zn}^{2+} > \text{Ni}^{2+} > \text{Mn}^{2+}$ for pH 5.

As mentioned above, because of stronger affinity for Pb^{2+} , retardation factors were larger than the other tested metals for both pH 4 and 5, and consequently the BTCs of Pb^{2+} were longer than others (Figures. 4.2a and 4.2b), and sorbed metal per gram soil of Pb^{2+} was higher than the other tested metals for both pHs (0.091 at pH 4 and 0.117 and 0.134 mmol g^{-1} at pH 5). Studies conducted by other have found that, Pb^{2+} has the strongest affinity to clays, peat, Fe-oxide, as compared to other metals (Jain and Ram, 1996; Sauve et al., 2000). As shown in Table 4.4, the retardation factors of these metals at pH 5 were higher than at pH 4 because there are less hydrogen ions (H^+) in the system at pH 5 than at pH 4 and, moreover, the Si-O⁻ and Al-O⁻ groups, the principal constituents of soils, are more protonated at pH 5 and, hence, they are more available sites, to retain the heavy metals in solutions (Esposito et al. 2001; Harter and Naidu, 2001; Abollino et al., 2003; Ponizovsky et al. 2003; Martínez-Villegas et al. 2004; Srivastava et al. 2005). As shown in Table 4.5 and Figure 4.3, the sorption capacities and retardation factors of Ni^{2+} were significantly greater than those of other heavy metals with increasing pH suggesting that the hydrolyzed form, which was affected by pH, may be more important in Ni^{2+} sorption. This result is in agreement with sorption of heavy metals of Brazilian soil, where sorption of Ni^{2+} was found to be positively correlated to pH, (Gomes et al., 2001). Additionally, as shown in Table 4.4 and Figure 4.2, results of the duplicated columns were similar showing consistency in column packing and experimental procedures.

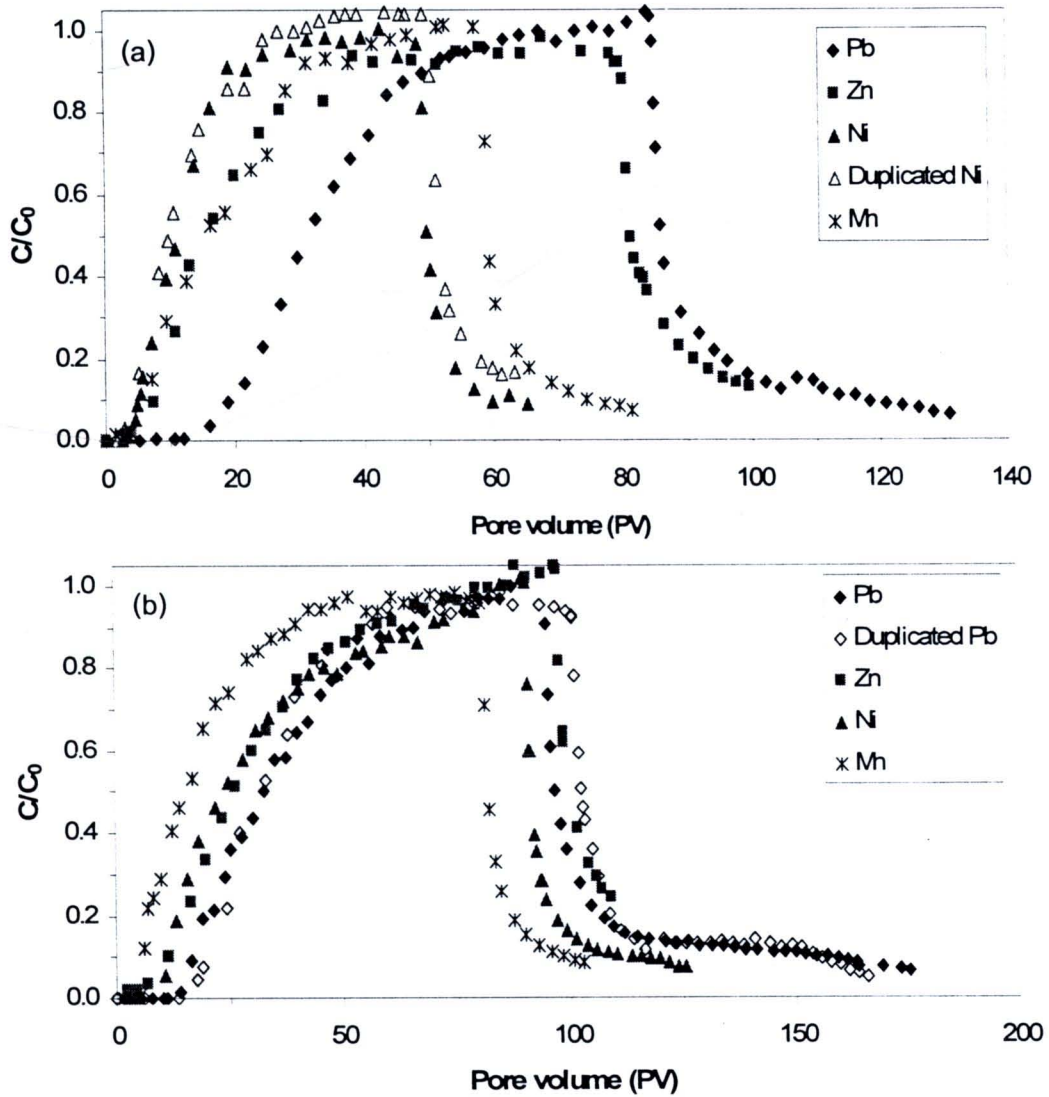


Figure 4.3 Experimental breakthrough curves of Pb^{2+} , Zn^{2+} , Ni^{2+} , and Mn^{2+} in lateritic soil at (a) pH 4 and (b) pH 5

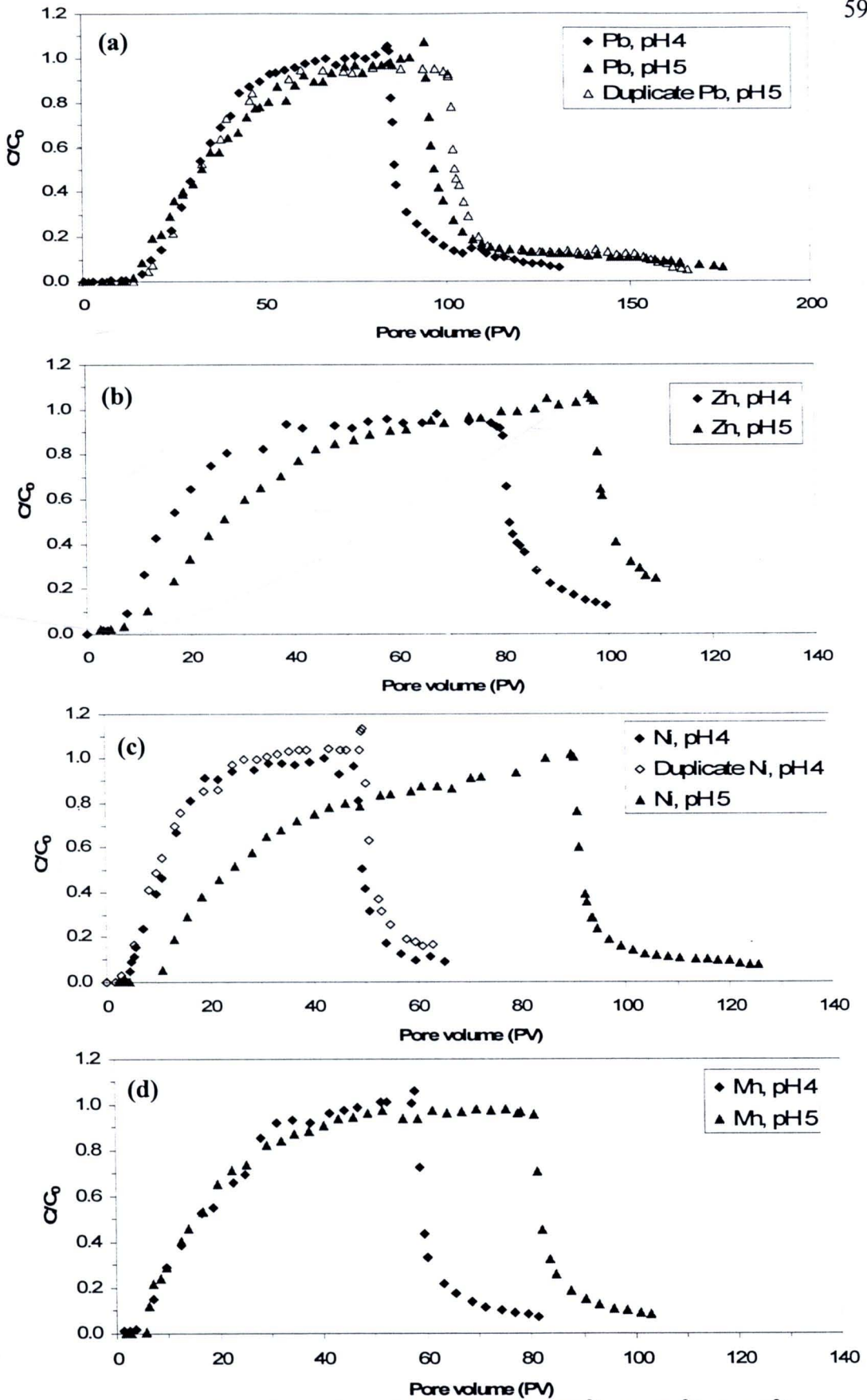


Figure 4.4 Effect of pH on breakthrough curves for (a) Pb^{2+} , (b) Zn^{2+} , (c) Ni^{2+} , and (d) Mn^{2+} in lateritic soil

Table 4.4 Summary of physical-chemical and sorption isotherm parameters of the lateritic column studies at pH 4 and 5.

<i>pH</i>	<i>Metal</i>	C_0^* (mM)	<i>L</i> (cm)	ρ ($g\ cm^{-3}$)	<i>n</i> ($cm^3\ cm^{-3}$)	<i>q</i> ($mL\ hr^{-1}$)	v ($cm\ hr^{-1}$)	R_{area}^\dagger	Sorbed /g soil ($mM\ g^{-1}$)	mass recovery (%)	<i>PV</i>
4	Pb ²⁺	5.28	10	1.03	0.62	7.65	2.52	33.26	0.091	73.47	28.42
	Zn ²⁺	4.67	10	0.96	0.65	8.15	2.57	19.61	0.069	82.91	30.48
	Ni ²⁺	5.06	10	1.10	0.59	7.54	2.61	11.22	0.036	92.56	27.19
	Ni ^{2+†}	5.28	10	1.03	0.62	7.53	2.48	11.21	0.043	91.18	33.49
	Mn ²⁺	4.87	10	0.93	0.66	7.97	2.47	17.90	0.067	79.87	31.49
5	Pb ²⁺	5.05	10	1.03	0.62	7.76	2.55	35.35	0.117	73.45	31.50
	Pb ^{2+†}	5.01	10	1.00	0.63	7.92	2.55	38.71	0.134	73.17	31.17
	Zn ²⁺	4.61	10	0.92	0.66	8.43	2.61	30.15	0.095	68.49	29.54
	Ni ²⁺	4.89	10	0.92	0.66	7.57	2.40	28.65	0.108	74.06	30.90
	Mn ²⁺	4.81	10	0.93	0.66	8.19	2.54	19.22	0.069	81.86	29.97

[†] Estimated from area method (Maraqa, M.A. 2001)

[‡] Duplicated column

* C_0 : initial concentration, *L*: column length, ρ : bulk density, η : porosity, *q*: flow rate, *v*: average pore-water velocity, *R*: retardation factor, *PV*: pore volume of the soil column

Table 4.5 Percentage increase in sorption capacity and retardation factors of heavy metals from pH 4 to pH 5

Metal	% increase	
	Sorption capacity	Retardation factor
Pb ²⁺	38.5	11.3
Zn ²⁺	37.7	53.8
Ni ²⁺	130.4	155.6
Mn ²⁺	3.00	7.4

4.3.3 Heavy metal transport – HYDRUS-1D Modeling results

Figures 4.4 and 4.5 show the experimental and simulated BTCs for Pb²⁺, Zn²⁺, Ni²⁺, and Mn²⁺ at pH 4 and 5 using HYDRUS-1D with linear sorption and nonlinear sorption equilibrium model and two-site model (TSM) (nonequilibrium model) to describe the main mechanisms controlling metal transport in lateritic soil. Table 4.7 summarized the estimated parameters for the metals using HYDRUS-1D.

4.3.3.1 Prediction of BTC using batch sorption data

Using sorption parameters (Q_{max} and b) derived from the batch tests (Putthividhya and Chotpantararat, 2007) and the dispersivity (λ) from the tracer test, HYDRUS-1D with the local equilibrium assumption (LEA) was applied to generate the predicted breakthrough curves of heavy metals at pH 4. The batch test sorption parameters are given in Table 4.6. As shown in Figure 4.4, the predicted heavy metals BTCs showed large deviations from experimental data, except for the duplicated column of Ni (SSE = 0.254). The predicted heavy metal BTCs using batch-determined sorption parameters were unable to describe the experimental data under pH 4 suggesting that the resident time in soil was not long enough for some sorption sites to reach equilibrium. The predicted Ni's BTC was better than the other metals predicted-BTCs which may be due to the less time needed to reach equilibrium conditions of Ni²⁺ than the other tested metals. Another explanation for the deviations

between the observed and predicted heavy metal BTCs may be due to the differences in soil:water ratios in batch and column experiments (Bürgisser et al., 1993). Unlike the bromide BTCs, heavy metals BTCs were asymmetrical and exhibited tailing, especially Pb^{2+} (See Figure 4.2 and 4.3). These results might be due to the presence of nonequilibrium processes in the system. According to bromide BTCs, the system was not influenced by physical nonequilibrium, suggesting that nonequilibrium conditions occurring in the lateritic soil column at this pore water velocity was primarily chemical nonequilibrium process. The observed nonequilibrium transport behavior was probably caused by rate-limited sorption.

Table 4.6 The batch sorption parameters at pH 4 from previous study (Putthividhya and Chotpantararat, 2007)

Metal	Langmuir sorption parameter		
	Q_{max} (mM g ⁻¹)	B (L mM ⁻¹)	R ²
Pb ²⁺	0.16±0.02	0.22±0.02	0.99
Zn ²⁺	0.14±0.02	0.19±0.06	0.97
Ni ²⁺	0.10±0.01	0.24±0.15	0.99
Mn ²⁺	0.08±0.01	0.26±0.07	0.96

4.3.3.2 Application of Linear and Langmuir isotherm using HYDRUS-1D with local equilibrium assumption

Using the local equilibrium assumption (LEA), linear and nonlinear Langmuir isotherm parameter estimation were performed to curve fit the heavy metal BTCs using HYDRUS-1D code as shown Figures 4.4 and 4.5. The SSE showed that Langmuir isotherm explained the experimental data better than the linear isotherm. This is similar to the batch tests showed where Langmuir isotherm was shown to fit well the batch tests data (Putthividhya and Chotpantararat, 2007). The Q_{max} values derived from batch tests were similar to those derived from fitting column experimental data using Langmuir isotherm but binding energy values (b) of these

metals derived from fitting the column experimental data were much greater than those obtained from batch tests (See Table 4.6 for batch tests and Table 4.7). Differences in the estimated b values for batch and column studies might be due to different of soil:water ratios in the system and different flow schemes in systems (closed and opened flow system for batch and column studies, respectively). Although the optimized BTCs using Langmuir isotherm fitted better than the linear isotherm, the curve-fitted BTCs using Langmuir isotherm showed sharp concentration fronts lagging the experimental data for pH 4 and 5.

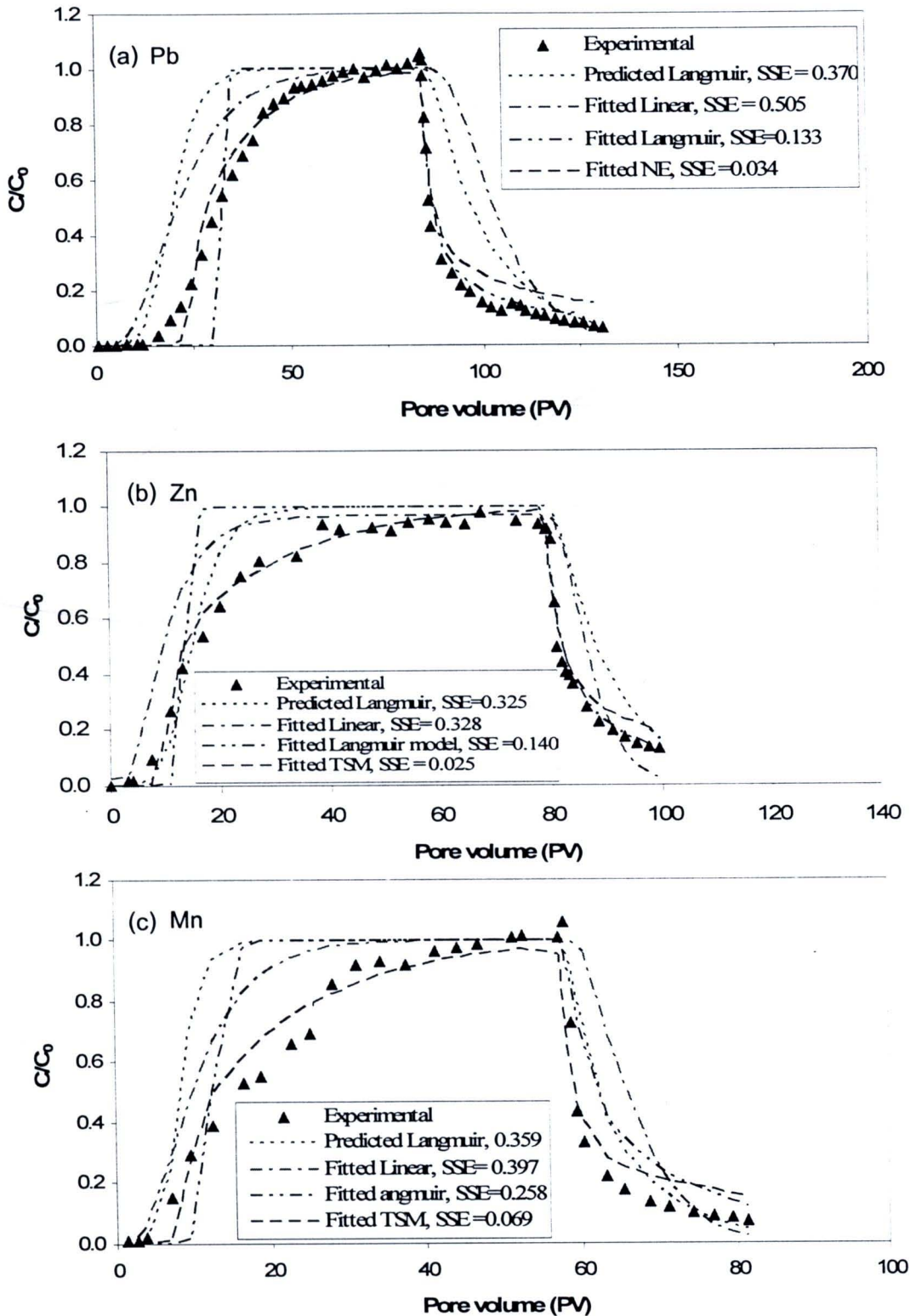


Figure 4.5 Heavy metal breakthrough data for lateritic soil at pH 4; (a) for Pb^{2+} , (b) for Zn^{2+} , (c) for Mn^{2+} , (d) for Ni^{2+} , and (e) for duplicated column of Ni^{2+} . Curves represent predictions of heavy metal concentrations using the convection-dispersion model (CDE) with independent parameters from batch experiments and tracer tests, optimized curve-fitting with linear and Langmuir isotherm, and the optimized curve-fitting with two-site model (TSM) model.

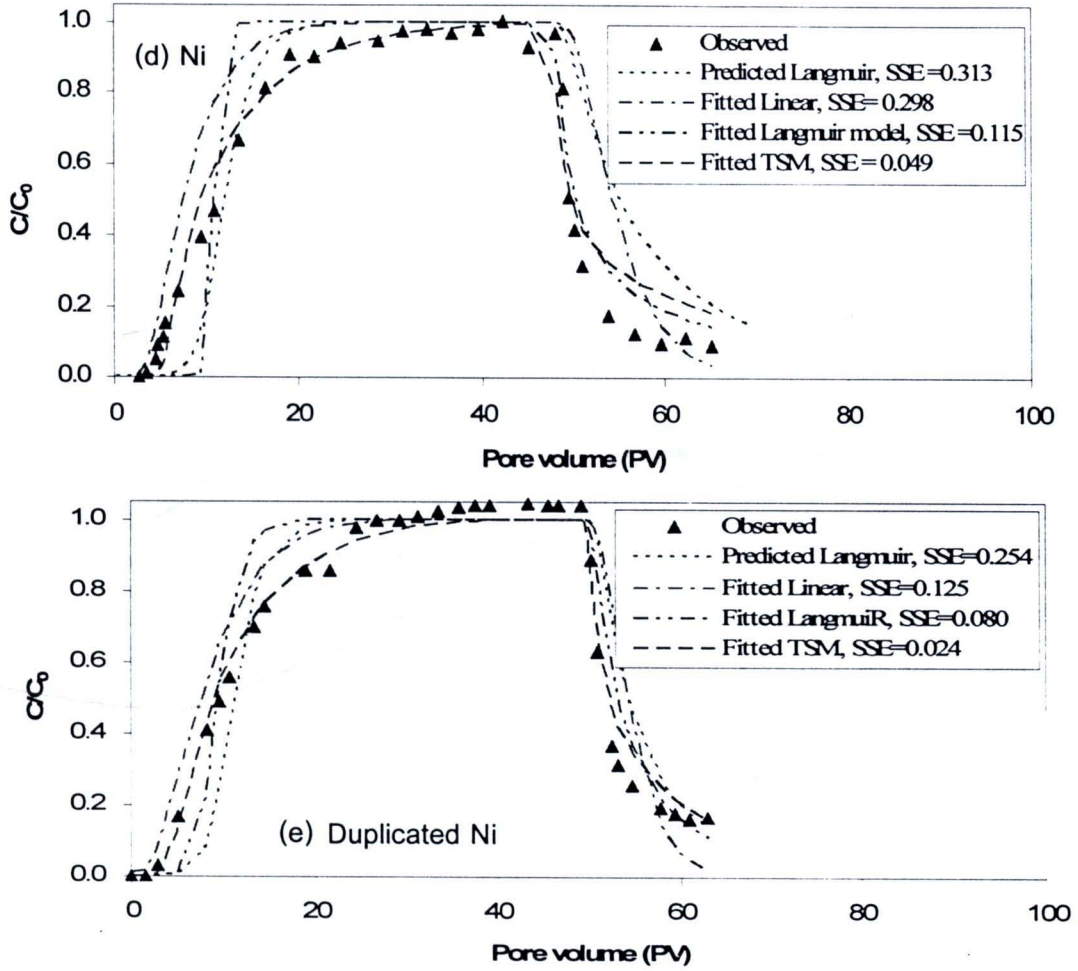


Figure 4.5 (Continue) Heavy metal breakthrough data for lateritic soil at pH 4; (a) for Pb^{2+} , (b) for Zn^{2+} , (c) for Mn^{2+} , (d) for Ni^{2+} , and (e) for duplicated column of Ni^{2+} . Curves represent predictions of heavy metal concentrations using the convection-dispersion model (CDE) with independent parameters from batch experiments and tracer tests, optimized curve-fitting with linear and Langmuir isotherm, and the optimized curve-fitting with two-site model (TSM) model.

The asymmetrical shape of metal BTCs especially the long tailings (as for Pb^{2+}) had been shown to be described better by a nonequilibrium transport model (Pang et al., 2002; Tsang and Lo, 2006).

4.3.3.3 Application of chemical nonequilibrium two-site model (TSM)

The two-site nonequilibrium approach has been explored for heavy metals to explain the failure of local equilibrium model to describe heavy metal BTCs in soils (Mclean and Bledsoe, 1992; Seuntjens et al., 2001; Pang et al., 2002; Jeon et al., 2004; Bellir et al., 2005). As mentioned above, the nonequilibrium is probably due to the kinetics of sorption occurring in the columns. As shown in Figures 4.4 and 4.5, the TSM could describe all of the BTC of heavy metals better than linear and Langmuir model based on LEA as seen by the SSEs at pH 4; $SSE_{TSM} (0.034) < SSE_{Langmuir} (0.133) < SSE_{Batch\ tests\ Langmuir} (0.370) < SSE_{Linear} (0.505)$. Applying the *t*-test on the average SSEs obtained from the chemical nonequilibrium two-site model and the convection-dispersion model with Langmuir isotherm, it was found that the curve-fitted results of the chemical non-equilibrium two-site model were significantly different from the equilibrium convection-dispersion model for pH 4 and 5 (*t*-test, $P < 0.05$), indicating that the fitted values by chemical nonequilibrium two-site model presented a better agreement with the experimental results (statistically significant, $P < 0.05$) than the equilibrium convection-dispersion model. Because of the heterogeneous nature of the lateritic soil, sorption to some surface may not be in equilibrium work done by Tsang and Lo (2006) found that metal cations (Cd^{2+} and Cu^{2+}) were spontaneously sorbed on exchangeable and carbonate fractions and was attained within 30 min but sorption on three other fractions (oxide, organic matter, and residual fractions) required much more reaction time (~ 7 days) to achieve equilibrium. The three fractions reflect rate-limited sorption behavior in system.

In Table 4.7, the maximum sorption capacities estimated by TSM: $Q_{max, Pb^{2+}} (0.15) > Q_{max, Zn^{2+}} (0.11) \sim Q_{max, Mn^{2+}} (0.10) > Q_{max, avg. Ni^{2+}} (0.07)$ for pH 4; and $Q_{max, Pb^{2+}} (0.20) \sim Q_{max, Zn^{2+}} (0.19) \sim Q_{max, Ni^{2+}} (0.18) > Q_{max, Mn^{2+}} (0.15)$ for pH 5. Pb^{2+} had the highest sorption capacity compared to the rest of other metals at both pH 4 and 5, which was in agreement with results of batch studies (Putthividhya and Chotpantararat, 2007) and retardation factors obtained by the area method. The fraction of instantaneous site (*f*) of all metals for the lateritic soil was consistently about 30-44

% of sorption site which may reflect the sand and silt fraction of the lateritic soil. Moreover, Pb^{2+} had the highest binding energy (b) as in both Langmuir model and TSM model which is in line with Pb^{2+} BTCs having long tailing and Pb^{2+} showing the lowest recovery (Table 4.4).

The TSM provided better prediction of the early tailing of the asymmetrical portion of heavy metal BTCs than the local equilibrium model but did not describe well the extended tailing of these heavy metals. It is probably that the rate of desorption can not be described by a first-order rate constant (Connaughton et al., 1993; Selim, 1999; Yamamoto et al. 2004) or it might be that more than one type of kinetic rates are needed in addition to the instantaneous sorption and first-order rate constant. Selim (1999) observed that sorption/desorption behavior of Cu^{2+} for a McLaren soil showed hysteresis behavior or nonsingularity at high concentrations, which could not be explained using first-order rate constant. In addition, the extended tailings may be controlled by mass transfer diffusion which was not accounted for in TSM (Beigel and Pietro, 1999). The kinetics of sorption/desorption along with hysteresis and/or mass transfer need to be further studied and, more precisely, represented for an accurate modeling and prediction of heavy metals transport through this soil. Based on the above analysis, use of the batch-determined sorption parameters would not be proper for elucidating the transport of heavy metals when the residence time in soil is not long enough to reach equilibrium.

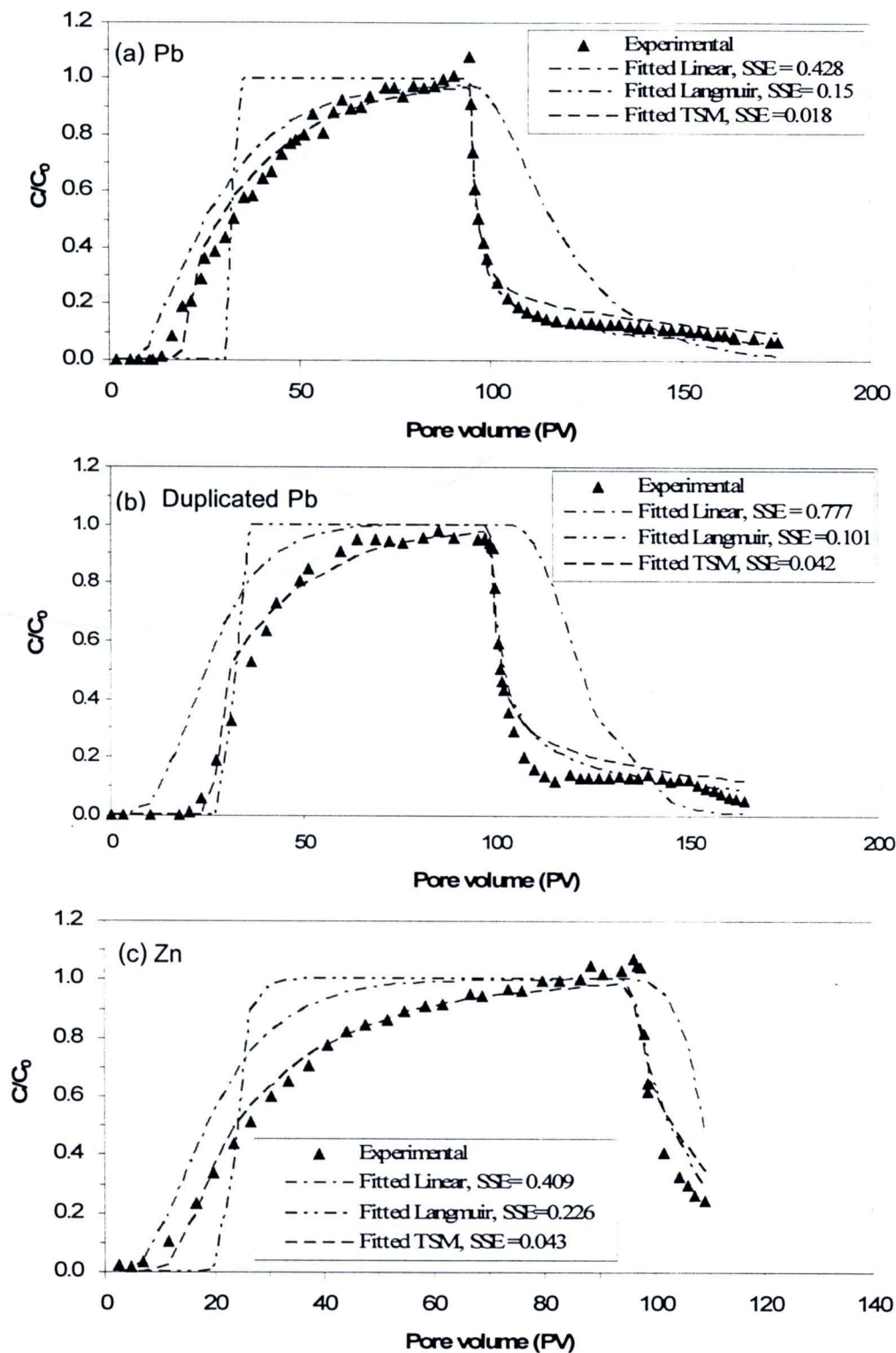


Figure 4.6 Heavy metal breakthrough data for lateritic soil at pH 5; (a) for Pb^{2+} , (b) for duplicated Pb^{2+} , (c) for Zn^{2+} , (d) for Mn^{2+} , and (e) for Ni^{2+} . Curves represent concentrations optimized curve-fitting with linear and Langmuir isotherm and the optimized curve-fitting with two-site model (TSM) model.

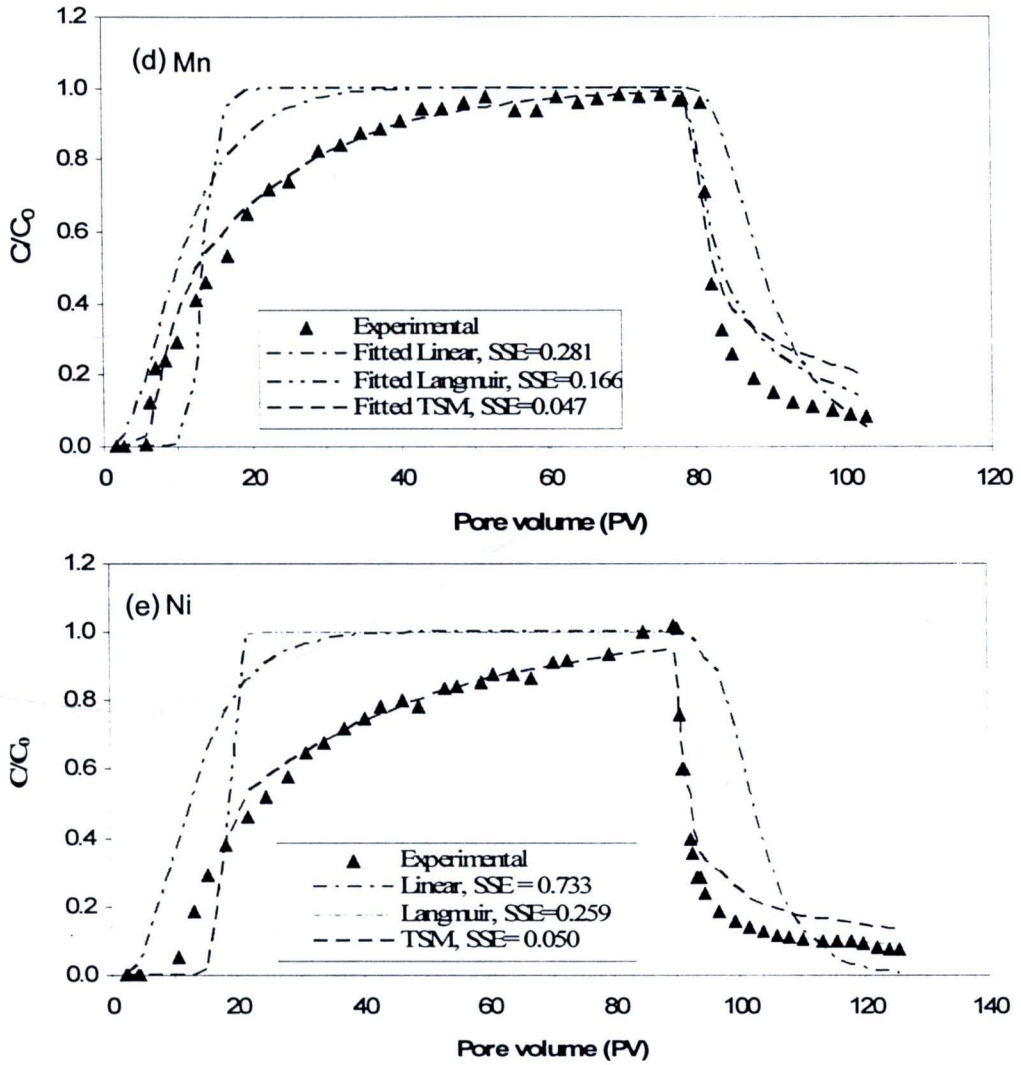


Figure 4.6 (Continued) Heavy metal breakthrough data for lateritic soil at pH 5; (a) for Pb^{2+} , (b) for duplicated Pb^{2+} , (c) for Zn^{2+} , (d) for Mn^{2+} , and (e) for Ni^{2+} . Curves represent concentrations optimized curve-fitting with linear and Langmuir isotherm and the optimized curve-fitting with two-site model (TSM) model.

Table 4.7 Estimated transport parameters for heavy metals (Pb^{2+} , Zn^{2+} , Ni^{2+} , and Mn^{2+}) breakthrough curve from equilibrium convection-dispersion and non-equilibrium approaches (2-site model) generated by HYDRUS-1D

No	pH	Metal	λ^{\ddagger} (cm)	Measured v (cm hr ⁻¹)	Equilibrium model fit				Nonequilibrium model fit					
					Linear		Langmuir		2-site (TSM)		2-site (TSM)			
					$K_d \pm 95\%CI$ (L g ⁻¹)	SSE	$Q_{max} \pm 95\%CI$ (mM g ⁻¹)	$b \pm 95\%CI$ (L mM ⁻¹)	SSE	$Q_{max} \pm 95\%CI$ (mM g ⁻¹)	$b \pm 95\%CI$ (L mM ⁻¹)	f $\pm 95\%CI$	$\alpha \pm 95\%CI$ (hr ⁻¹)	SSE
1		Pb ²⁺	1.42	2.52	20.40±0.04	0.428	0.16±0.03	6.71±1.03	0.133	0.15±0.03	2.95±0.57	0.44±0.16	0.018±0.007	0.036
2		Zn ²⁺	1.42	2.57	9.45±0.02	0.328	0.07±0.03	1.69±0.76	0.114	0.11±0.04	1.09±0.76	0.40±0.06	0.016±0.006	0.025
3	4	Ni ²⁺	1.42	2.61	6.46±0.06	0.298	0.05±0.01	1.82±0.24	0.115	0.06±0.03	0.90±0.39	0.35±0.11	0.039±0.023	0.049
4		Ni ²⁺ (Dup.)	1.42	2.48	7.54±0.08	0.125	0.06±0.03	0.38±0.10	0.080	0.08±0.03	0.44±0.19	0.44±0.05	0.039±0.018	0.024
5		Mn ²⁺	1.42	2.47	11.25±0.02	0.397	0.08±0.02	0.83±0.13	0.253	0.10±0.02	1.78±0.39	0.33±0.14	0.019±0.010	0.069
6		Pb ²⁺	1.42	2.58	20.39±0.01	0.428	0.17±0.01	10.75±0.21	0.148	0.20±0.04	3.34±0.78	0.31±0.05	0.011±0.001	0.020
7		Pb ²⁺ (Dup.)	0.96 [†]	2.55	24.53±0.01	0.765	0.16±0.07	6.09±2.42	0.104	0.20±0.04	2.39±0.54	0.42±0.12	0.012±0.005	0.044
8	5	Zn ²⁺	1.42	2.61	20.31±0.05	0.344	0.13±0.06	1.34±0.33	0.226	0.19±0.03	0.65±0.10	0.41±0.05	0.016±0.003	0.043
9		Ni ²⁺	1.42	2.40	12.81±0.01	0.733	0.09±0.09	4.24±3.49	0.259	0.18±0.02	2.94±0.38	0.34±0.03	0.008±0.001	0.050
10		Mn ²⁺	1.73 [†]	2.54	11.53±0.01	0.281	0.08±0.04	1.26±0.80	0.166	0.12±0.03	0.80±0.26	0.33±0.06	0.018±0.007	0.047

[†] dispersivity derived from tracer test ; [±] average dispersivity derived from average of dispersivity values of 3 tracer columns

4.4. Conclusion

Experimental BTCs of four heavy metals showed that Pb^{2+} had the highest sorption capacity and retardation factor of the 4 metals at pH 4 and 5. The sorption capacity of heavy metals increase with increasing pH due to competition between hydrogen ions and metals as the aluminol and silanol groups become more protonated for higher pH. The sorption capacity and retardation factors of Ni^{2+} were found to increase significantly greater than those of other heavy metals when the pH was changed from 4 to 5 suggesting that the hydrolyzed form of Ni^{2+} , which was affected by pH, may be more important in Ni^{2+} sorption.

The symmetrical shape of the Br^- BTC and estimated parameters of two region model ($\beta = 1$ and $\omega \geq 100$) of the lateritic soils suggested the absence of physical nonequilibrium for the column studies. The asymmetrical shape of the heavy metals with long tailing (especially Pb^{2+}) of heavy metal BTCs indicate chemical nonequilibrium conditions during heavy metals transport through the lateritic soil.

Batch derived sorption parameters used with HYDRUS-1D did not describe the experimental BTCs for pH 4 and 5, suggesting non-equilibrium condition. When the column experimental data were curve fitted by linear and nonlinear Langmuir isotherm (local equilibrium assumption) and the two-site nonequilibrium model (TSM), the TSM described BTCs better than the equilibrium linear and Langmuir model. The curve-fitted results of the TSM chemical nonequilibrium two-site model were found to be statistically different from the results of the equilibrium convection-dispersion model indicating that the TSM presented a better agreement with the experimental results (statistically significantly, $P < 0.05$). However, TSM could not describe well the extended tailing of these heavy metals which may be due to the rate of sorption/desorption which is different from a first-order rate constant.

From the TSM model, the order of estimated Q_{max} and retardation factors for the four metals were $\text{Pb}^{2+} > \text{Zn}^{2+} \sim \text{Mn}^{2+} > \text{Ni}^{2+}$, indicating that Pb^{2+} will be retarded the most through the lateritic soils. The estimated fraction of instantaneous sorption was between 0.30 to 0.44 for four metals and pH 4 and 5, indicating that nonequilibrium sorption exist for the bulk of the surfaces.